

Luminescent properties and energy level structure of CaZnOS:Eu²⁺

Budde, B.; Luo, H.; Dorenbos, P.; van der Kolk, E.

DOI

[10.1016/j.optmat.2017.04.045](https://doi.org/10.1016/j.optmat.2017.04.045)

Publication date

2017

Document Version

Accepted author manuscript

Published in

Optical Materials

Citation (APA)

Budde, B., Luo, H., Dorenbos, P., & van der Kolk, E. (2017). Luminescent properties and energy level structure of CaZnOS:Eu²⁺. *Optical Materials*, 69, 378-381. <https://doi.org/10.1016/j.optmat.2017.04.045>

Important note

To cite this publication, please use the final published version (if applicable).
Please check the document version above.

Copyright

Other than for strictly personal use, it is not permitted to download, forward or distribute the text or part of it, without the consent of the author(s) and/or copyright holder(s), unless the work is under an open content license such as Creative Commons.

Takedown policy

Please contact us and provide details if you believe this document breaches copyrights.
We will remove access to the work immediately and investigate your claim.

Luminescent Properties and Energy Level Structure of CaZnOS:Eu^{2+}

B. Budde¹, H. Luo¹, P. Dorenbos¹, E. van der Kolk^{1*}.

¹Delft University of Technology, Faculty of applied Sciences, Department radiation Science and technology, Luminescent Materials Research Group, Mekelweg 15, 2629 JB, Delft, The Netherlands.

*Corresponding author: E.vanderKolk@tudelft.nl

Abstract

In this work it is shown that CaZnOS:Eu^{2+} has no Eu^{2+} emission even at low temperature. The observed and earlier reported red emission originates from a CaS:Eu^{2+} impurity phase. By means of washing the as-prepared samples with diluted nitric acid, we are able to remove the CaS impurity and get the pure CaZnOS . A clear relation was found between the red emission intensity, the CaS XRD line intensities and the nitric acid solution washing time, with zero intensity after prolonged washing. Later, a so-called VRBE (vacuum referred binding energy)-diagram was constructed showing the energy of the $4f^n$ and $4f^{n-1}5d^1$ states of the divalent and trivalent rare earth ions as dopants in CaZnOS with respect to the vacuum energy. This diagram shows that the 5d-levels of Eu^{2+} are located in the conduction band, which explains the absence of $5d \rightarrow 4f$ emission. By comparing the VRBE diagram with diagrams of other related compounds like CaO , CaS , ZnO and ZnS it becomes clear that the Eu^{2+} luminescence quenching is caused by a low lying conduction band, typical for Zn-based compounds.

1. Introduction

Red light emitting phosphors are of interest for their applications in white light-emitting diodes[1] and are considered for their potential to increase the rate of photosynthesis in algae systems[2, 3]. LEDs are energy efficient light sources that have found a wide range of applications since their discovery. Currently the most common method to produce white LEDs is by combining a blue LED chip (450-470 nm) with a yellow phosphor[3]. This however gives a cold white light and in order to produce a warmer colour of light a red emitting phosphor is needed. When Eu^{2+} is doped in a proper host lattice it is known to accommodate this red light emission[4].

The emission of Eu^{2+} arises from a $5d \rightarrow 4f$ transition. As the 5d electronic level is not shielded from the surrounding ligands[5], its energy varies widely with the lattice in which the Eu^{2+} ions are doped and is determined by the combined effect of the centroid shift and the crystal field splitting of the 5d states. The centroid shift is the lowering of average energy of the 5d states compared to a free ion. The centroid shift is larger when Eu is coordinated by S ions compared to O ions because it follows the nephelauxetic series[6]. The crystal field splitting is caused by the electron repulsion between the 5d states and the surrounding ligands and is therefore affected by the size and symmetry of the Eu lattice site.

CaS:Eu^{2+} is a commercially available red phosphor emitting at a maximum of 650nm. CaZnOS:Eu^{2+} has been reported to emit red luminescence that is practically the same as CaS:Eu^{2+} [3, 7]. In this article the two materials will be compared because it is not expected that two significantly difference between Eu lattice sites in CaS and CaZnOS

would give the same emission. A detailed analysis of phase pure Eu^{2+} , Eu^{3+} and Yb^{3+} doped CaZnOS powder samples will lead to the conclusion that CaZnOS:Eu^{2+} does not have Eu^{2+} emission and that the red emission accredited to CaZnOS:Eu^{2+} originates from a small quantity of CaS:Eu^{2+} impurity phase.

2. Experimental methods

CaZnOS has been synthesized by the following reaction: $\text{ZnS} + \text{CaO} \rightarrow \text{CaZnOS}$. The synthesis of pure phase CaZnOS is challenging because of the decomposition reaction above 1370 K: $\text{CaZnOS} \rightarrow \text{ZnO} + \text{CaS}$. Additionally ZnO easily decomposes to O_2 gas and Zn vapor when heated above 1205 K under reducing atmosphere[8], and this decomposition is accelerated by the presence of carbonate salts such as CaCO_3 [9]. Above 1180 K ZnS and CaO (i.e. CaCO_3 after thermal decomposition) react towards CaS and ZnO , which in time decomposes to zinc vapor[10]. Since a reducing environment is required when Eu_2O_3 is used as a starting material the synthesis towards a pure phase CaZnOS:Eu^{2+} is difficult because a small CaS phase is almost always present. Nevertheless several studies on CaZnOS report a pure phase without CaS impurities [3, 11, 12]. In this research, obtained CaZnOS samples were successfully purified by washing with a solution of water and nitric acid, a method not yet used for CaZnOS . With this method a series of CaZnOS:Eu^{2+} phosphors with decreasing CaS content was synthesized to investigate the luminescent properties as a function of the amount of CaS impurity.

For the synthesis of CaZnOS:Eu^{2+} , CaCO_3 (99.95%, Alfa Aesar), ZnS (99.99%, Alfa Aesar) and Eu_2O_3 (99.99%, Sigma Aldrich) were weighted in stoichiometric quantities and extensively ground with a pestle and mortar and placed in an Al_2O_3 crucible which was placed in a larger crucible and heated at 900°C for 32 hours under a 7% H_2 / 93% N_2 reducing atmosphere in a tube furnace and subsequently cooled down to room temperature. For the undoped CaZnOS host an 8-hour reaction time was used at the same conditions. The doping concentration of Eu was 4 mol%. The CaS:Eu^{2+} was obtained as a commercial product from Intematix. The washing of the product was performed by adding a 1% nitric acid solution of water to the sample, followed by stirring, filtration and washing with acetone. For the synthesis of the Eu^{3+} doped pure phase CaZnOS , the host lattice was synthesized first. After that, Eu_2O_3 was added in the as-prepared CaZnOS and re-annealed at the same temperature for 4 hours in the N_2 atmosphere.

The XRD measurements were performed by a PANalytical XPert Pro XRD spinner between a 2θ value of 5° and 80° in a 1-hour measurement. The radiation source is a $\text{Cu K}\alpha$ anode at 45 kV and 40 mA with $\lambda(\text{K}\alpha_1) = 0.154060$ nm and $\lambda(\text{K}\alpha_2) = 0.154443$ nm. The background determination was performed with Highscore software. Emission spectra were recorded of powder samples that were compressed to pills and placed in a rotating sample holder to minimize any effects from sample holder displacement. Sample were excited by a monochromatic Expla OPO laser and the emission spectra were collected with an Ocean Optics QE65000 Spectrometer. For low temperature measurements, spectra were obtained by pelletizing the sample and irradiated with a 150W Xenon arc lamp (Hamamatsu L2273). A Gemini 180 Monochromater was used to tune the excitation wavelength. The emission spectra were obtained by an Acton Sp2300 Spectrometer. The excitation spectra were calibrated by the Xe lamp spectrum and the emission spectra were calibrated by the detector response curve. Diffuse reflection spectra were obtained by placing the sample in a sample holder and irradiating it with an Acton Deuterium lamp. The reflection spectra were measured by

an Ocean Optics QE65000 Spectrometer. BaSO₄ was used as a reference for the reflection measurement.

3. Results

In Figure 1 the XRD spectra of four samples are presented: (a) CaZnOS (washed), (b) CaZnOS:Eu²⁺ (unwashed), (c) CaZnOS:Eu²⁺ (washed) and (d) CaS:Eu²⁺. Spectra (a) and (d) show the same lines as the reference spectra for CaZnOS and CaS obtained from the Pearson's Crystal Database[13]. Many peaks of CaS overlap with those of CaZnOS, however the peak at 45° is unique for CaS and is therefore considered the best indicator to determine the amount of CaS impurity phase within the CaZnOS samples.

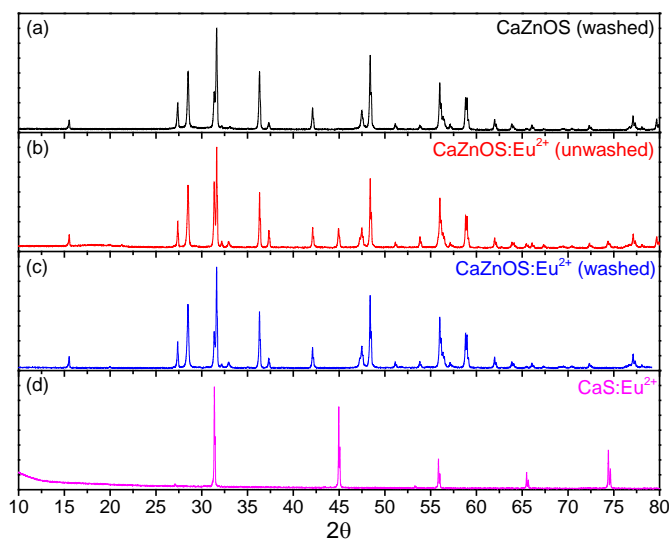


Figure 1. XRD spectra of : (a) CaZnOS (washed), (b) CaZnOS:Eu²⁺ (unwashed) , CaZnOS:Eu²⁺ (washed) and (d) commercial CaS:Eu²⁺.

In Figure 2, a close-up of the 45° peak in the XRD spectra of a series of CaZnOS samples with increasing washing time is presented to demonstrate the decreasing CaS line at 45°. The CaZnOS:Eu²⁺ samples are labelled 1 through 4 referring to the unwashed (spectrum 4), the once washed (3), and the thrice washed (2) sample. Sample (1) was washed until a pure phase CaZnOS was obtained.

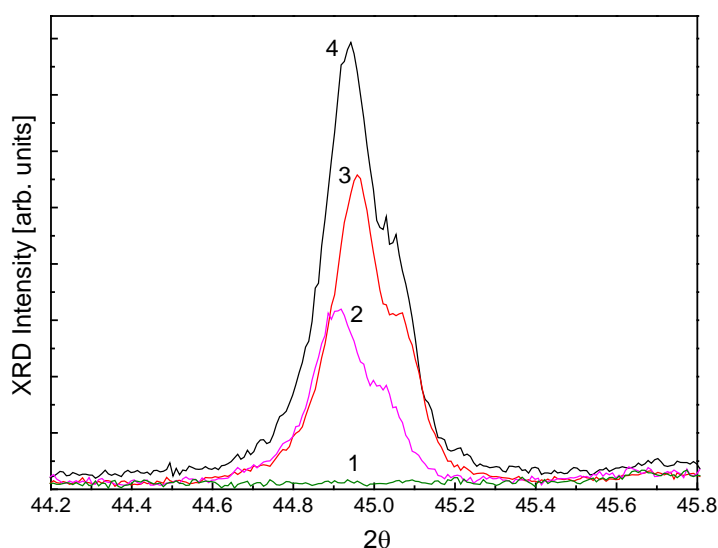


Figure 2. Zoom in on the 45° XRD peak intensity as a function of washing time for the unwashed (4), once washed (3) and thrice washed (2) sample. Sample (1) was washed until a pure phase CaZnOS was obtained.

A comparison between the optical properties of CaZnOS (washed), CaZnOS:Eu²⁺ (unwashed), pure phase CaZnOS:Eu²⁺ (washed) and CaS:Eu²⁺ was made. In Figure 3 the diffuse reflection spectra of the four samples are presented. An absorption band between 400 and 600 nm in CaS is clearly visible in spectrum labelled 4 as expected. No Eu-related absorption bands can be seen in the undoped CaZnOS sample (spectrum 1). The phase pure CaZnOS:Eu²⁺ sample shows an absorption band peaking at 380nm as can be seen from spectrum 3. We assign this band to 4f→5d absorption by Eu²⁺ in CaZnOS. The absorption features of the unwashed CaZnOS:Eu²⁺ sample (spectrum 2) of which the XRD spectra has shown that it contained CaS:Eu²⁺, can nicely be explained by a combination of bands due to Eu²⁺ in CaS and CaZnOS. Spectra were not plotted beyond 600 nm as the measured diffusely reflected light was too much contaminated with the red luminescence from Eu²⁺. This can already be seen from the too high diffuse reflection values for spectrum 2 towards 600 nm. Spectra 1, 2, and 3 have a short wavelength absorption onset near 280-290nm that marks the fundamental absorption onset E_{fa} . An additional absorption band marked A for spectra 1 and 3 has unknown origin.

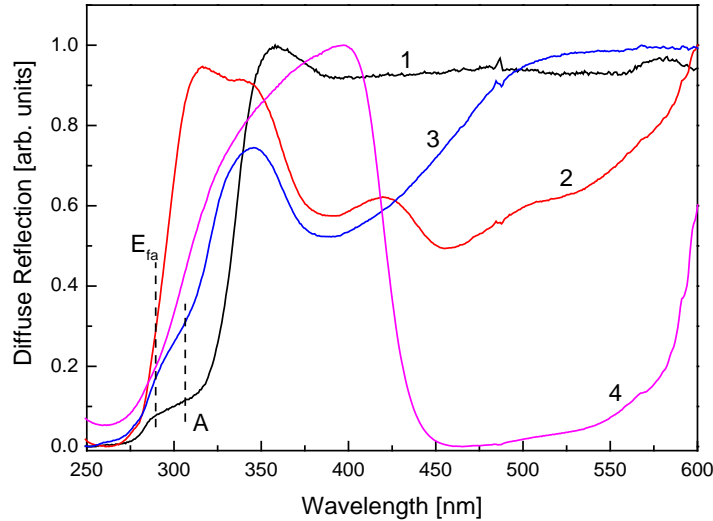


Figure 3. Normalized diffuse reflection spectra for CaZnOS (black curve labelled 1), CaZnOS:Eu²⁺ with CaS:Eu²⁺ (red curve labelled 2), CaZnOS:Eu²⁺ (blue curve labelled 3) and CaS:Eu²⁺ (purple curve labelled 4).

In Figure 4 the emission of the four samples with decreasing CaS phase is presented under 500 nm laser excitation in the absorption band of Eu²⁺ in CaS:Eu²⁺. The intensity of emission decreases rapidly with decreasing CaS content.

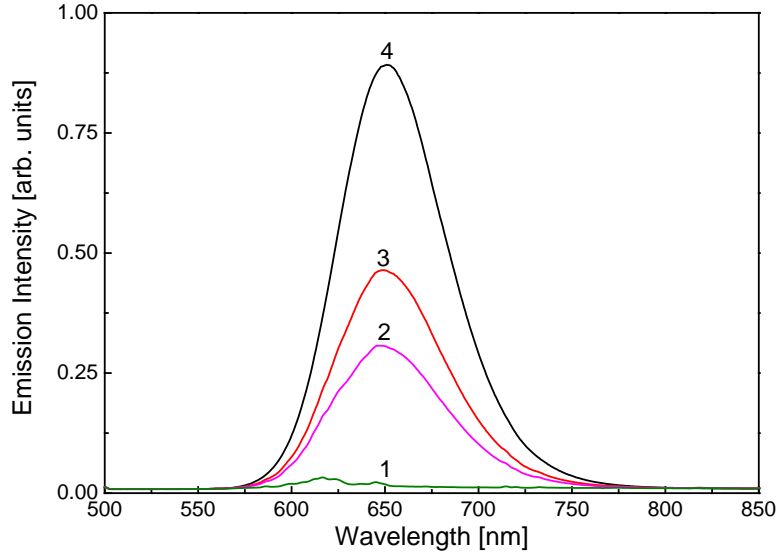


Figure 4. Emission spectra excited at 500 nm for the unwashed (4), once washed (3), and thrice (2) washed samples. Sample (1) was washed until a pure phase CaZnOS was obtained.

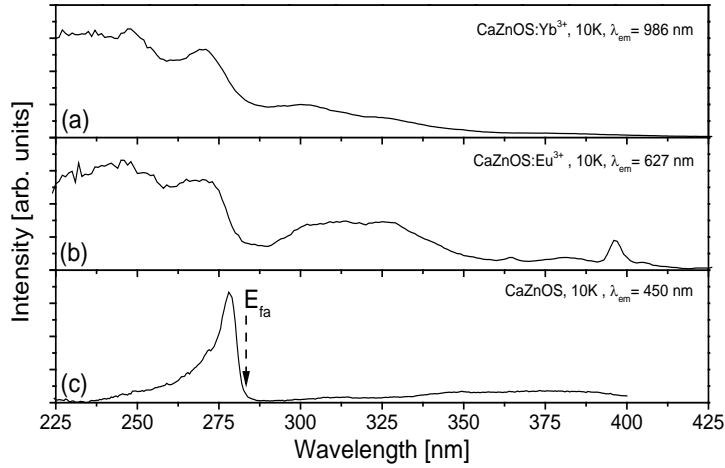


Figure 5. Luminescence excitation spectra of CaZnOS:Yb³⁺ (a), CaZnOS:Eu³⁺ (b) and undoped CaZnOS (c).

We did not observe any luminescence on excitation in the 380nm 5d absorption band of CaZnOS, not even at 10K. Such absence can be explained when the lowest energy 4f⁶5d excited state of Eu²⁺ is located close or above the conduction band bottom[14]. In order to verify this, luminescence excitation spectra were recorded on samples doped with Eu³⁺ and Yb³⁺ to obtain the VB→Ln³⁺ charge transfer energies of these ions as well as an undoped sample to obtain the exciton- and bandgap energy of CaZnOS. These energies can be used to construct a so-called vacuum referred binding energy diagram (VRBE) that provides the location of all lanthanide ground and excited states and the host valence band and conduction band states with respect to the vacuum level. All samples were washed and free from any CaS impurity phase. The results are presented in Figure 5.

Figure 5b shows the excitation spectra of 627 nm Eu³⁺ emission at 10K. The 0.55 eV broad band at 315 nm (3.9 eV) is attributed to the valence band to Eu³⁺ charge transfer (CT) transition. At 270 nm (4.6 eV) the host exciton band is observed. This peak can be observed more clearly in the undoped sample of Figure 5c when monitoring host-related emission at 10 K around 450nm. This onset of this peak near 285 nm is the optical bandgap or fundamental absorption threshold E_{fa} of CaZnOS. The energy agrees

with the absorption band onset found for CaZnOS:Eu²⁺ in the diffuse reflection spectra of Figure 3. The optical bandgap of CaZnOS is reported in literature with different values between 3.7 and 4.3 eV[11-13]. The bandgap of CaS is reported at 4.9 eV[15]. The CT-band of Yb³⁺ is always expected at about 0.4 eV higher energy than that of Eu³⁺ [16] and is therefore anticipated at 288 nm. Figure 5a shows the excitation spectrum monitoring the 4f_{5/2}→4f_{7/2} emission of Yb³⁺. Besides the host exciton band at 275 nm a broad band centred around 300 nm (4.2 eV) is observed within an acceptable range of the predicted value.

4. Discussion

The experimental data presented in this work strongly suggest that the 650 nm emission that was accredited to CaZnOS:Eu²⁺ [3, 7, 12] is actually from samples that contain small quantities of a CaS:Eu²⁺ impurity phase. CaZnOS:Eu²⁺ samples that are washed with nitric acid solution have no longer any XRD lines characteristic for CaS nor have any red emission at 650 nm. Also the diffuse reflection spectrum of a washed and phase pure CaZnOS:Eu²⁺ sample does not have the characteristic absorption bands of Eu²⁺ in CaS between 400 and 600 nm but instead it has a band at much shorter wavelength peaking at 380nm (3.3 eV).

Based on the collected spectroscopic data presented above, the vacuum referred binding energy diagram for CaZnOS can be constructed. The energy-values used to construct the diagram in Figure 6 are indicated by the vertical arrows 1, 2, 3 and 4 that represent the host exciton creation energy of 4.5 eV, the 4f⁷→4f⁶[⁷F₀]⁵d¹ energy of 2.6 eV, the Eu³⁺ and Yb³⁺ CT energies respectively. The energy difference between the Eu²⁺ ground state and Eu³⁺ ground state, the so-called U-value in the chemical shift model, [17, 18] was taken as 6.4 eV which is the average of the values that pertain to CaO, ZnO, CaS, and ZnS presented below. The electron-hole binding energy in the host exciton is assumed to be about 4% of the exciton creation energy. It is evident that the lowest 5d state of Eu²⁺ in CaZnOS is well above the bottom of the conduction band, which implies that upon excitation of the 5d state, the electron will immediately delocalise into the conduction band without Eu²⁺ 5d→4f emission even at 10 K.

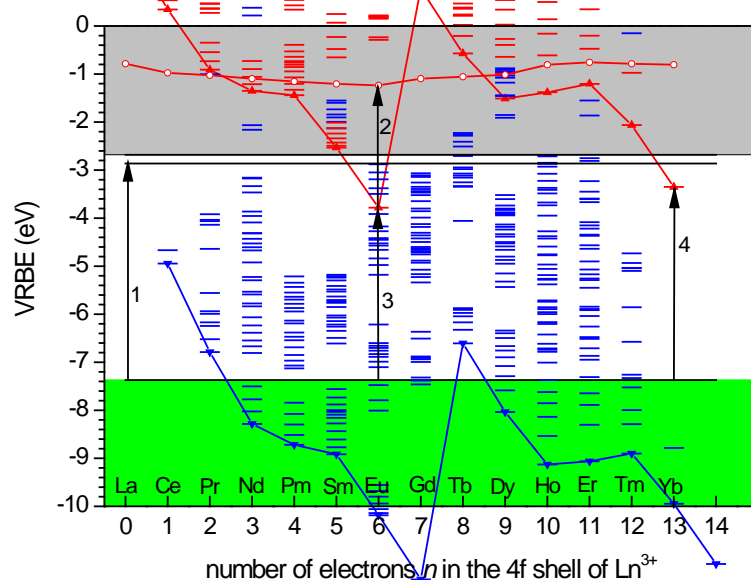


Figure 6. VRBE diagram for CaZnOS. The vertical arrows indicate the experimentally determined energies that were used to construct this diagram.

It is instructive to compare the VRBE-diagrams of the related compounds CaO, CaS, ZnO, ZnS and CaZnOS.

The VRBE-diagrams of CaS and ZnO were published earlier [19, 20]. In electrochemistry the top of the valence band for ZnS is at about 2.36 eV below the H^+/H_2 redox potential [21] which brings it at -6.8 eV on the VRBE scale. We further used the 3.86 eV for the host exciton creation energy with an exciton binding energy of 40 meV from Hoshina *et al.* [22]. In CaO the exciton creation peak is at 6.94 eV [23] and the VB→Eu³⁺ charge transfer band near 250nm (4.96 eV)[24-26]. For the U-parameter a value of 6.3 eV was assumed and the $4f^7 \rightarrow 4f^6[{}^7F_0]5d^1$ energy is 1.85 eV[24].

In figure 8 we present the VRBE diagrams stacked next to each other. It shows the top of the valence band, the VRBE in the Eu²⁺ $4f^7$ ground state and when available in the $4f^6[{}^7F_0]5d^1$ state, the VRBE in the host exciton state and at the bottom of the conduction band. The conduction band bottom for CaZnOS falls in between that for ZnO and CaS. Something similar applies to the top of the valence band. For sulfides it is usually at -6 eV and for oxides between -8 eV and -9 eV. The top of the valence band in CaZnOS falls in between that of a CaS and CaO or ZnS and ZnO.

From a study of Eu in more than 100 different compounds it was found that the VRBE in the lowest 5d state is on average near -1 eV with a tendency to decrease with smaller value for the U-parameter[27]. The level locations for CaO, CaZnOS and CaS in Figure 7 agree with that finding. The absence of Eu²⁺ emission in CaZnOS is then caused by a low lying conduction band bottom like in ZnO. On replacing oxygen for sulphur the conduction band moves upward. For ZnS Eu²⁺ emission is still not observed, but interestingly the Eu²⁺ emission starts to appear for nanosized particles where due to band gap widening the conduction band moves to above the the Eu²⁺ 5d-level [28].

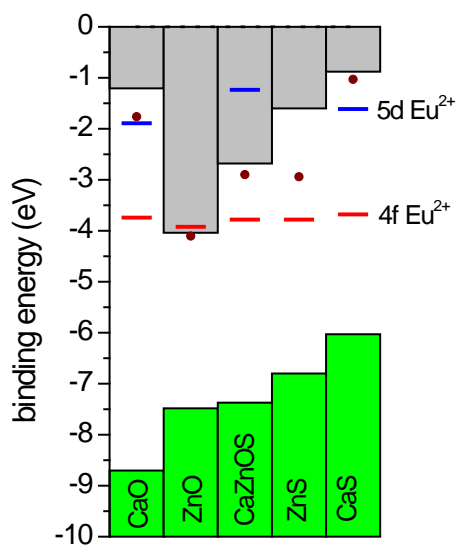


Figure 7. Energy levels of Eu²⁺ in CaO, ZnO, CaS and ZnS

The low lying conduction band in ZnO as compared to CaO, and in ZnS as compared to CaS means that the electron is stronger bonded in the 4s conduction band orbital of Zn as compared to the 4s CB orbital of Ca. This reflects the atomic properties where the 2nd ionisation potential of Zn (17.96 eV) is much higher than that of Ca (11.57 eV).

5. Conclusion

Based on the presented experimental results it can be concluded that CaZnOS:Eu^{2+} has no luminescence as the Eu^{2+} 5d states are located in the conduction band. The red emission accredited to Eu^{2+} in CaZnOS in literature is in fact emission from Eu^{2+} in a CaS impurity phase that can be washed out using acid water.

References

- [1] C.C. Lin, R.-S. Liu, J. Phys. Chem. Lett., 2 (2011), pp. 1268-1277.
- [2] L. Wondraczek, M. Batentschuk, M.A. Schmidt, R. Borchardt, S. Scheiner, B. Seemann, P. Schweizer, C.J. Brabec, Nat. Commun., 4 (2013).
- [3] T.-W. Kuo, W.-R. Liu, T.-M. Chen, Opt. Express, 18 (2010), pp. 8187-8192.
- [4] P.F. Smet, A.B. Parmentier, D. Poelman, J. Electrochem. Soc., 158 (2011), pp. R37-R54.
- [5] B. Grabmaier, Luminescent materials, Springer Verlag 1994.
- [6] P. Dorenbos, J. Lumin., 136 (2013), pp. 122-129.
- [7] Z. Qiu, C. Rong, W. Zhou, J. Zhang, C. Li, L. Yu, S. Liu, S. Lian, J. Alloys Compd., 583 (2014), pp. 335-339.
- [8] R. Gulyaeva, E. Selivanov, A. Vershinin, V. Chumarev, Inorg. Mater., 42 (2006), pp. 897-900.
- [9] H.-C. Hsu, C.-I. Lin, H.-K. Chen, Metallurgical and Materials Transactions B, 35 (2004), pp. 55-63.
- [10] C. Huang, C. Lin, H. Chen, J. Mater. Sci., 40 (2005), pp. 4299-4306.
- [11] C. Duan, A. Delsing, H. Hintzen, Chem. Mater., 21 (2009), pp. 1010-1016.
- [12] Z.-J. Zhang, A. Feng, X.-Y. Chen, J.-T. Zhao, J. Appl. Phys., 114 (2013), p. 21351801-21351808.
- [13] T. Sambrook, C.F. Smura, S.J. Clarke, K.M. Ok, P.S. Halasyamani, Inorg. Chem., 46 (2007), pp. 2571-2574.
- [14] P. Dorenbos, J. Phys.: Condens. Matter, 17 (2005), p. 8103-8111.
- [15] W.M. Yen, M.J. Weber, Inorganic phosphors: compositions, preparation and optical properties, CRC Press 2004.
- [16] P. Dorenbos, J. Phys.: Condens. Matter, 15 (2003), p. 2645-2665.
- [17] P. Dorenbos, Phys. Rev. B., 85 (2012), p. 165107.
- [18] P. Dorenbos, ECS J. Solid State Sci. Technol., 2 (2013), pp. R3001-R3011.
- [19] D.C. Rodríguez Burbano, S.K. Sharma, P. Dorenbos, B. Viana, J.A. Capobianco, Adv. Opt. Mater., 3 (2015), pp. 551-557.
- [20] P. Dorenbos, ECS J. Solid State Sci. Technol., 3 (2014), pp. R19-R24.
- [21] A. Kudo, Y. Miseki, Chem. Soc. Rev., 38 (2009), pp. 253-278.
- [22] T. Hoshina, H. Kawai, Jpn. J. Appl. Phys., 19 (1980), p. 279-287.
- [23] R. Whited, W. Walker, Phys. Rev. Lett., 22 (1969), p. 1428.
- [24] N. Yamashita, J. Electrochem. Soc., 140 (1993), pp. 840-843.
- [25] M. Kang, X. Liao, Y. Kang, J. Liu, R. Sun, G. Yin, Z. Huang, Y. Yao, J. Mater. Sci., 44 (2009), pp. 2388-2392.
- [26] A. Mayolet, J. Krupa, I. Gerard, P. Martin, Mater. Chem. Phys., 31 (1992), pp. 107-109.
- [27] E. Rogers, P. Dorenbos, ECS J. Solid State Sci. Technol., 3 (2014), pp. R173-R184.
- [28] W. Chen, J.-O. Malm, V. Zwiller, R. Wallenberg, J.-O. Bovin, J. Appl. Phys., 89 (2001), pp. 2671-2675.